Proceedings of the
International Conference on Mechanical Engineering and Renewable Energy 2011
(ICMERE2011) 22- 24 December 2011, Chittagong, Bangladesh

ICMERE2011-KI-I

CHARACTERISTICS OF TEMPERATURE RISE IN PRACTICAL HYDROGEN PRESSURE TANKS BEING FILLED AT HIGH PRESSURE OF 35 AND 70 MPa

M. MONDE[1]
[1] Institute of Ocean Energy, Saga University
1 Honjo-machi, Saga, 840-8502, Japan
E-mail:monde@me.saga-u.ac.jp

Abstract- *A model is proposed by Monde et al. to estimate hydrogen temperature in the tank during filling the hydrogen tank. Some experimental data sets, not only on the hydrogen temperature within the tank during filling, but also on the supplied temperature and pressure from the station have been opened for analysis of the temperature change with time in order how to supply hydrogen in its tank safely in a market. The data were independently obtained for some different conditions and have been analyzed and checked to validate the model. It is found that the measured temperatures are well predicted using the software based on the model and the heat loss during filling with hydrogen is also well predicted, if a suitable heat transfer coefficient is adopted.*

Keywords: Hydrogen tank for fuel cell vehicle, Fast filling, Pressure vessel, Temperature rise during filling at high pressure

1. INTRODUCTION

Recently, it was decided that the first phase of commercial fuel cell vehicles (FCV) will be introduced to the market from 2015 as the first phase by Japanese automotive companies [1, 2]. Corresponding to their activities, the Japanese government has started financially supporting construction of about 100 hydrogen stations in four major economical areas in Japan. In order to successfully complete this project by 2015, one has to understand the temperature characteristics of hydrogen in the tanks. Temperature control is as one of the key technologies, because the temperature of the hydrogen during filling hydrogen up to 70 MPa into the carbon fiber reinforced plastic (CFRP) composite tank should be limited to lower than 85 °C due to a safety regulation. More recently, filling tests have been extensively executed to keep this regulation for several different kinds of tanks. Some of the results, which have been measured during filling hydrogen into the tank by private companies are gradually entering the open literature for analysis of the temperature characteristics. In other countries, there are also many research projects on hydrogen storage at high pressure in concert with Japanese activities as well as overseas automotive activities.

According to experimental results, when a hydrogen vessel is filled on a hot summer's day and/or using a fast filling procedure up to 70 MPa, unfortunately, the temperature in the tank can go beyond 85 °C. Therefore, the supplied hydrogen should be highly cooled so as not to exceed the hydrogen temperature of 85 °C and more precise temperature behavior in the tank should be required from a better understanding and safety points of view.

With the above circumstances in mind, many experiments and numerical studies have been conducted to grasp the temperature behavior in the tank during fast filling with hydrogen fast into the tank at high pressure [3-12]. Monde et al. [3] measured the temperature change during filling of a small tank with hydrogen and nitrogen to a pressure of 30 MPa and then showed the temperature distribution and effects of the filling time and location of the nozzle on the temperature distribution. In addition, they showed that the highest temperature hydrogen appears near the opposite end of the tank to the nozzle and how the heat transfer coefficient changes with mass flow rate was guantified. Monde et al. [3, 4] proposed a thermodynamic model together with heat transfer from hydrogen into the tank wall, by which the measured temperatures during fast-fill study up to 35 and 70 MPa conducted at Powertech in Canada were analyzed [4]. Their study yielded agreement in the trends of temperature behavior for both 35 and 70 MPa between the measured and estimated ones, but poor quantitative agreement for 70 MPa. The poor agreement at 70 MPa may be caused by a lack of thermal properties and specifications of the tank.

Dicken and Merida [5] conducted an elaborate experiment by arranging 63 thermocouples distributed throughout the tank to capture the temperature profile. They showed that the temperature field within the cylinder was significantly stratified in the vertical direction for slower fills and then, the except for the region near the wall and the injected zone, the temperature seemed to change almost uniformly. Dicken

and Merida [6] proposed a numerical model based on symmetric flow where the effects of gravitational and buoyancy forces are ignored in comparison with the velocity effect. The temperature estimated by their model seems to be in poor agreement with the measured values. Liu et al. [7] also measured the temperature change during refueling hydrogen vessels and showed the effects of initial pressure and mass velocity on the temperature rise.

Some researchers [8,9,10] numerically analyzed the temperature distribution during filling of hydrogen tanks using the CFD codes and compared the measured temperature rise by Dicken and Merida [5] with the estimated one during the increase in mass. It is hard to say that the agreement between them is good. Maus et al. [11] and Zheng et al. [12] discussed a procedure to refuel hydrogen at a practical hydrogen station.

Incidentally, New Energy Development Organization (NEDO) [1, 2] in Japan has financially supported us in order to expand a FCV society smoothly, and in particular to construct several hydrogen stations, what is required to refuel hydrogen into the FCV is safely becoming clear. Through Japan Hydrogen & Fuel Cell Demonstration Project (JHFC) and NEDO activities including of support of automotive companies, the measured data not only of the hydrogen temperature within the tank during filling with hydrogen but also on the supplied temperature and pressure from the station have been gradually opened for analysis of the temperature change with time. The present paper analyzes these available data to validate the Monde et al. model [3, 4] and then shows a comparison between the estimated and measured temperatures. In addition, what kinds of physical parameters mainly influence the temperature rise will be discussed.

2. THERMODYNAMIC MODEL FOR REFUELING OF HYDROGEN TANK

The refueling process of the tank surely obeys the first law of thermodynamics for a semi-open system as shown in Fig. 1 and is given without any work in a form of time derivative as follows:

$$dU/dt = dQ/dt + h_{in}dm_{in}/dt \qquad (1)$$

Where U is the total internal energy of the tank, Q is the heat added to the system from the surroundings and h_{in} is the enthalpy at the inlet and m_{in} is the supplied mass to the tank.

In order to solve Eq.(1), one has to evaluate the heat transfer rate dQ/dt between hydrogen and the tank and the internal energy throughout the tank, while the value of $h_{\mathrm{in}}dm_{\mathrm{in}}/dt$ will be calculated from the refueling condition at the station. The value of dQ/dt can be given as:

$$\frac{dQ}{dt} = \int_A -\lambda \frac{\partial T_s}{\partial x}\Big|_{x=0} dA = \int_A \alpha_h (T_w - T_g) dA \qquad (2)$$

where T_g is the local temperature within the tank, T_s is the solid temperature, α_h is heat transfer coefficient, and A is the total inside surface area of the tank. The total internal energy is also given using the hydrogen density ρ_g and specific internal energy u_g as:

$$\frac{dU}{dt} = \frac{d}{dt}\int_V \rho_g u(p,T_g) dV \qquad (3)$$

where V is the total inside volume of the tank. The density in the tank is given by the real-gas equation of state specified in Eq. (4). The compressibility, Z, is calculated using a polynomial fit to hydrogen gas data generated the Lee-Kesler method [14]. This data agreed well with tabulated compressibility data [15] for hydrogen in the range of temperatures considered in this study.

$$\rho(P,T_g) = \frac{P}{Z(P,T_g)RT_g} \qquad (4)$$

The specific internal energy is also calculated from the hydrogen gas data [14].

2.1 Evaluation of local temperature in the tank

According to the measurements by Dicken and Merida [5] of the hydrogen temperature using 63 thermocouples distributed throughout the cylindrical tank with a straight nozzle, the temperature field within the cylinder was significantly stratified in the vertical direction for slower fills and then the temperature change took place almost uniformly, except for the region near the wall and the injected zone. In the case of a fast fill, a large temperature distribution is created by the injected hydrogen from a straight nozzle and a hot spot is observed near the area opposite the inlet nozzle. Similar temperature behavior was also observed by Monde et al. [3] and was numerically shown by Heitsch et al. [8]. Recently, in order to avoid the generation of the hot spot, a specially designed nozzle has been attached in place of the straight nozzle, by which the hydrogen can be uniformly expanded throughout the tank and then the temperature distribution is made smooth and the temperature rise is also made uniform.

Assuming that the hydrogen is well stirred within the tank and its temperature is uniformly increased over the tank, that is, the values of ρ_g and u_g are constant through the tank, one can rearrange Eq. (3) as follows:

$$\frac{dU}{dt} = \frac{d}{dt}\int_V \rho_g u(p,T_g) dV = V\frac{d}{dt}(\rho_g(p,T_g)u(p,T_g)) \qquad (5)$$

Also Eq.(2) can be simplified as follows:

$$\frac{dQ}{Adt} = -\lambda \frac{\partial T_s}{\partial x}\Big|_{x=0} = \alpha_h (T_w - T_g) \qquad (6)$$

Equation (6) is the boundary condition coupling hydrogen and liner.

2.2 Evaluation of heat transfer between hydrogen and tank wall

As the heat transfer coefficient α_h in Eq. (2) is generally given by a function of the flow situation and thermal conductivity, it may locally change with time. Woodfield et al. [13] measured the local heat transfer

coefficient when gas has been filled into a model tank through a straight nozzle and proposed a correlation predicting the heat transfer coefficient. They showed that the values of a_h varied from 400 to 700 W/(m^{2}K) depending on the change of a slow fill to fast fill. In addition, Woodfield et al. [4] showed that the temperature rise, which was measured during a filling hydrogen up to 35 MPa for a type III tank with a straight nozzle, can be well predicted using the value of α_h = 500 W/(m^{2}K) by the Monde et al. model [3, 4]. However, for the case of an advanced tank with a different kind of nozzle, the heat transfer coefficient of α_h = 500 W/(m^{2}K) is found to be quite large, since the nozzle is designed to spread the hydrogen within the tank as uniformly as possible and hence the expected value becomes smaller than about α_h = 200 W/(m^{2}K) which will be discussed later.

From the heat transfer point of view, it may be worth mentioning that if the Biot number, $\alpha_h\delta/\lambda_s < 0.1$, then heat conduction in a solid can be treated as lumped capacity heat flow, that is the temperature distribution in the solid appears almost uniform across the thickness, δ. As example, we evaluated the Biot number for type III and IV tanks with liner thickness of δ = 3 mm, resulting into $\alpha_h\delta/\lambda_s$ = 0.003 and = 0.51 for α_h = 200 W/(m^{2}K), respectively. For the type III tank, the temperature can be treated to be uniform in the Al liner parallel to the heat flow direction. In addition, the high thermal conductivity would make the temperature difference perpendicular to the heat flow direction, which is caused by the local fluctuations of the hydrogen temperature and of the heat transfer coefficient, flat over the liner thickness. For the type IV with $\alpha_h d/\lambda_s$ = 0.51, on the other hand, some effect of these local fluctuations surely remains when compared with the type III. Therefore it is important, particularly for type IV vessels, to consider the temperature distribution across the wall thickness.

2.3 Deployment of thermodynamic model together with heat conduction

Figure 1 gives an overview of the present model [4]. Substituting Eqs. (2), (3) and (5) into Eq. (1), one can obtain the following equation:

$$V\frac{d}{dt}(\rho_g(p,T_g)u(p,T_g)) = A\alpha_h(T_w - T_g) + h_{in}dm_{in}/dt \quad (7)$$

together with mass conservation, which is given as follows:

$$V\frac{d}{dt}(\rho_g(p,T_g)) = dm_{in}/dt \quad (8)$$

The wall is assumed to behave as a one-dimensional solid, thus conservation of energy to determine the wall temperature may be described by unsteady heat conduction, namely Eq. (9).

$$\frac{\partial T_s}{\partial t} = a_s\frac{\partial^2 T_s}{\partial x^2} \quad (9)$$

The boundary conditions for Eq. (9) are given by Eq. (10)

$$-\lambda_s\frac{\partial T_s}{\partial x}|_{x=0} = \alpha_h(T_g - T_s|_{x=0}) \quad (10\text{-a})$$

$$-\lambda_s\frac{\partial T_s}{\partial x}|_{x=l} = \alpha_e(T_s|_{x=l} - T_e) \quad (10\text{-b})$$

Here $T_w \equiv T_s|_{x=0}$ and l is the total thickness of the wall. The initial condition is taken to be a uniform temperature. It should be mentioned that the temperature and heat flux at the interface between liner and FRP have the identical values for both solids and the thermal properties are also used for the liner and FRP, respectively.

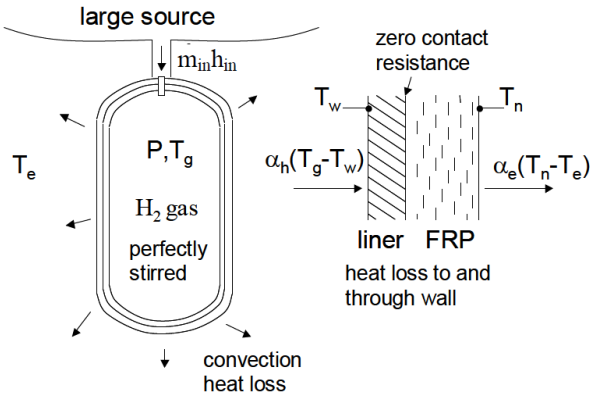

Fig. 1 Schematic diagram of thermodynamic model

2.4 Filling test of hydrogen

Woodfield et al. [4] conducted their experiment to verify the proposed model. In the experiment, the positioning of the thermocouples in the test vessel is shown in Fig.2. The details of experimental equipment and its measuring procedure were described in Ref. [4] The hydrogen is refueled through supply tanks at high pressures initially at 35 MPa. The gas temperature inside the vessel is measured using four thermocouples and the outside wall temperature using two thermocouples. Thermocouples TA and TE have different hot-junction diameters and are located at approximately the same position to check the effect of the response time of the sensor. For the filling rates investigated in the present study thermocouples TA and TE gave very similar readings indicating that the ordinary diameter thermocouples were small enough. Pressures and temperatures of the filling system, surrounding environment and test vessel are monitored simultaneously during each test run.

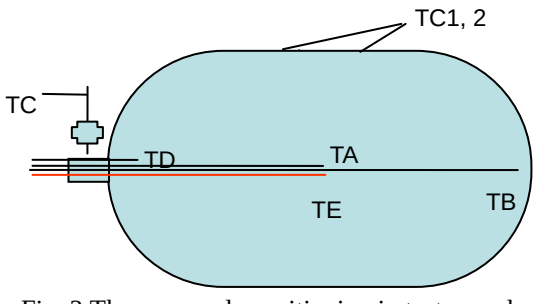

Fig. 2 Thermocouple positioning in test vessel
(TA, TB, TC, TD: ordinary diameter thermocouples)

Figure 2 shows the measured temperature rise during the filling hydrogen at 35 MPa and also calculated temperature rise. The tank specification and its thermal properties needed in the estimation are summarized in Table 1 and heat transfer coefficients for inside and outside of the tank are assumed to be 400 and 4.5 W/m^{2}K, respectively. It reveals from Fig. 2 that the agreement between model predictions and experiment is quite good on the whole, while the measured temperatures at the different positions are slightly different. Woodfield et al. pointed out that rather than using the measured inlet temperature changing with time, an effective constant inlet temperature was used so that the average inlet enthalpy matched the measured inlet condition.

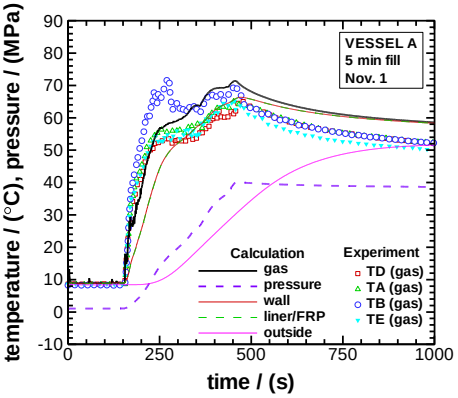

Fig. 3 Comparison between measured and estimated temperatures.

Table 1 Specification and thermal properties

Pressure/MPa	35	
Volume/L	205	
Area/m^2	2.33	
CFRP thickness/mm	17	
Liner thickness/mm	4.25	
Material	CFRP	AL liner
Conductivity/Wm^{-1}K^{-1}	0.55	180
Diffisivity/m^{2}s^{-1}	0.45 x 10^{-6}	74.4 x 10^{-6}
Density/kgm^{-3}	1530	2700

2.5 Concerning parameters for hydrogen filling process

As there are many parameters associated with the filling process as given by several concerned equations, it may be worth determining how many independent parameters are required to describe the process completely, before starting calculation. Therefore, we apply the π theorem to the process parameters, resulting into the following non-dimensional functional form against non-dimensional hydrogen temperature.

$$T_g{}^*(\tau) = f(\tau, Bi_1, Bi_2, \Pi_1, \Pi_2, \Pi_3, \Pi_4, \Pi_5) \quad (11\text{-a})$$

and also the temperature in the tank wall can be determined by adding dimensionless parameters related to the position as:

$$T^*(\tau,\xi) = f(\tau,\xi, Bi_1, Bi_2, \Pi_1, \Pi_2, \Pi_3, \Pi_4, \Pi_5) \quad (11\text{-b})$$

where dimensionless parameters are defined as $T^*= T/T_o$, $\tau = a_2 t/\delta_2{}^2$, $\xi = x/\delta_2$, $Bi_1 = \alpha_h\delta_2/\lambda_2$, $Bi_2 = \alpha_e\delta_2/\lambda_2$, $\Pi_1= A\delta_2/V$, $\notin_2 = (\rho c\delta)_2/(\rho c\delta)_1$, $\Pi_3 = (m_{in}h_{in}/\rho_o V h_o)\delta_2{}^2/a_2$, $\notin_4 = (\rho c)_2 T_o/\rho_o h_o$, and $\Pi_5 = p_o/\rho_o h_o$. It may be worth mentioning that number of the parameters concerned with the filling process is mainly 17 quantities, for example for a composite tank with two layers, which are reduced into independent dimensionless parameters by the π theorem. Except for 17 quantities, the specification of the inlet nozzle and the hydrogen properties are concerned. However, the effect of these parameters is indirectly taken through heat transfer coefficient into account. It should be noted that as the specific enthalpy strongly depends on its temperature, the enthalpy can be replaced by the temperature. The dimensionless parameter Π_1 is a parameter relating the tank shape and the tank dimensions, only. Therefore, different tanks with the identical value of Π_1 are considered as identical. It should be noted that ten dimensionless parameters are concerned with the filling process into the tank with two composite materials and are necessary and sufficient to describe the thermal characteristics.

Provided that the configuration of the tank, its thermal properties of liner and CFRP, and the heat transfer coefficients on the inside and outside of the tank are already known, then each independent dimensionless parameter can be separated and reformed into a group of dimensional ones. As a result, Eq. (11) for the gas temperature can be reformed into another form including six physical parameters, that is: initial condition (initial temperature T_o and initial pressure p_o), and final condition (T_f and p_f), filling time t and filling gas temperature T_{in}, as follows:

$$f(p_o, T_o, p_f, T_{f,} t, T_{in}) = 0 \quad (12)$$

It should be noticed that number of controlled parameters concerned with filling process of a given tank becomes six. In addition, the configuration of the tank, its thermal properties of liner and CFRP have the fixed values for the specified tank, while the heat transfer coefficients strongly depends on the flow situation within the tank and generally changes with time during filling process. As for heat transfer coefficient, incidentally, Woodfield et al. [13] measured the average heat transfer coefficient during filling into a small tank and discharging gas from the tank. They [13] mentioned that during filling hydrogen, the heat transfer coefficients vary from 100 to around 450 W/m^{2}K depending on filling mass flow rate from 0.1 to 0.6 g/s, and then their values are strongly influenced by the locations and is increased as the location becomes farther from the inlet. Ranong et al. [17] numerically estimate heat transfer coefficients during filling the process and showed that the estimated

values are in a range between 100 and 300 W/m^{2}K depending on the filling time.

2.6 Procedure to solve equations (7) to (10)

From Eq. (12), the system of equations is closed by specifying the measured pressure p_f and temperature T_f in the tank as a function of time until the tank is full for any combination of (p_o, T_o , T_{in} ,t) provided that some information on the tank specifications and thermal properties and then heat transfer coefficients of α_h and α_e on both surfaces of the tank wall are given. Therefore, we can calculate the temperature $T_g(t)$ during filling hydrogen for the specified tank, because most of the fill tests have been carried out for a combination of (p_o, T_o , p_f, T_{in} ,t). Monde and Woodfield have developed software for this calculation in which the inlet enthalpy can be directly calculated from the inlet transient temperature and then by which the estimated temperature $T_g(t)$ can be determined within 10 s on a conventional PC. It may be worth noting that the developed software can be equally applied to a discharge of gas, for which the sign of mass flow in Eq. (6) becomes negative and the enthalpy leaving the tank, h_{in} is calculated based on the instantaneous temperature and pressure in the vessel.

3. ANALYTICAL RESULT AND DISCUSSION

Recently, some data measured in the hydrogen filling tests financially supported by NEDO and JARI have been made available for analysis to estimate the thermal behavior. The measured data for four different tanks with different characters have been analyzed for a total of six tested initial conditions and filling times. The details of the needed specifications and properties of the tank are omitted here due to a space. The heat transfer coefficient α_h for the inside of the tank is changed by taking the filling time and mass flow rate into account, while the heat transfer coefficient for the outside of the tank, α_e is fixed at α_e = 4.5 W/m^{2}K for any calculation, although its value has almost no effect on the heat transfer.

Figures 4 to 9 show the measured and calculated temperatures together with the precooled temperature of the supplied hydrogen, rate of pressure increase and mass flow rate. The filling test up to 35 MPa is shown in Fig.4 and the others up to 70 MPa are given in Figs. 5 to 9.

Finally, it should be noted that the available temperature does not correspond to the actual gas temperature at the tank inlet except for the Runs #1 and #2, because the temperature sensor by which the temperature was measured, usually was located far from the tank inlet. Unfortunately, no information on how far the sensor was located away from the tank inlet is included in the data. Therefore, the true temperature at the tank inlet surely becomes higher than the given inlet temperature. The difference between them strongly depends on their distance and other conditions such as filling time, surrounding temperature and insulation conditions. According to author's estimation, the difference in the temperature between them may drop within a band of 5 to 10 K.

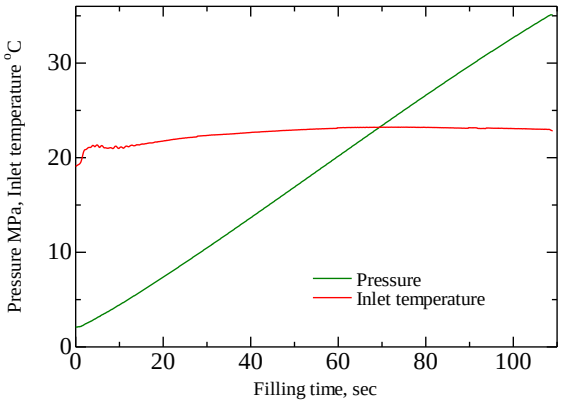

Fig. 4(a) Input data in filling test

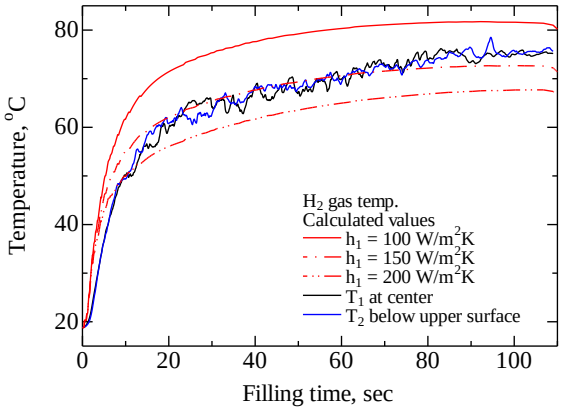

Fig. 4(b) Comparison between measured and estimated temperatures up to 35 MPa for type III with 34 L (Run #1)

3.1 Comparison between measured and estimated temperatures

Figure 4(a) shows a measured inlet temperature of about 22 °C and measured pressure in 34 L test tank during continuous filling to 35 MPa, and also Fig. 4(b) shows the measured temperatures at the center and below the upper surface of the tank and calculated results for different heat transfer coefficients of α_h = 100 to 200 W/m^{2}K. It may be noticed from Fig. 4(b) that both the temperatures at two different locations are increasing with time and are also fluctuating within the same temperature band, although the measured locations are different. This small temperature fluctuation may indicate that the hydrogen in the tank is well stirred. It is found from Fig. 4(a) that the calculated temperature using the value of α_h = 150 W/m^{2}K agrees well with the measured temperature except for the first 10 s.

Figure 5(a) shows a measured inlet precooled temperature of about - 20 °C and measured pressure in the 31 L test tank (Run #2) during continuous filling to 70 MPa, and also Fig. 5(b) shows the measured temperatures at the center and below the upper surface of the tank and calculated results for different heat transfer coefficients of α_h = 100 to 200 W/m^{2}K. It may be noticed from Fig. 5(b) that like Fig. 4(b), both the temperatures at

two different locations are increasing with time and are fluctuating within the same temperature band. It is found from Fig. 5(b) that the calculated temperature with agrees well with the measured temperatures, especially the temperature at the center. Both temperatures show a different trend near the end of fill. The buoyancy effect becomes more prominent, resulting into the different temperature behavior, since near the end of filling the stirring effect gradually disappears. It should be noticed that the value of = 200 W/m^{2}K is recommended for filling up to 70 MPa, while the value of α_h = 150 W/m^{2}K up to 35 MPa. The main reason that the different α_h values are recommended is that the mass flow rate up to 70 MPa becomes larger than that up to 35 MPa at the almost same filling time, namely, due to effect of the inlet velocity.

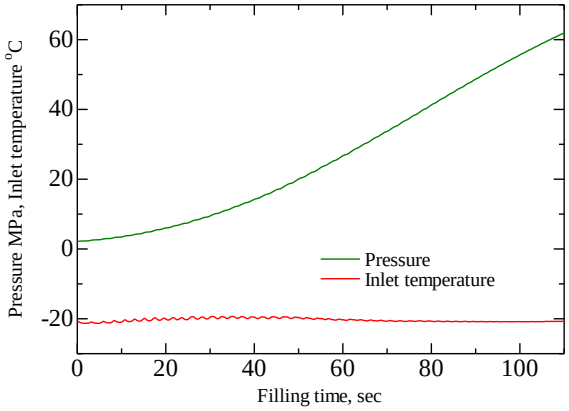

Fig. 5(a) Input data in filling test

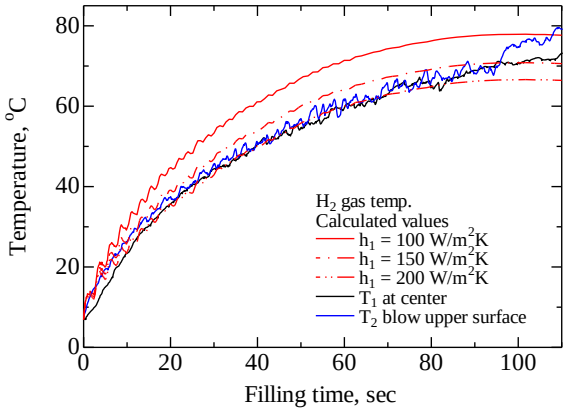

Fig. 5(b) Comparison between measured and estimated temperatures up to 70 MPa for type IV with 31 L (Run #2)

Figure 6(a) shows a measured inlet precooled temperature ranging from about - 20 to - 30 °C and measured pressure in the 31 L test tank during filling to 70 MPa using three hydrogen banks, and also Fig. 6(b) shows the measured temperatures for four identical tanks filled simultaneously and calculated results using different heat transfer coefficients of α_h = 100 to 200 W/m^{2}K. It is revealed from Fig. 6(b) that although the four tanks are identical, each measured temperature has a slightly different trend. This difference might be due to different inlet velocities and may be acceptable within the tolerance of the measuring system. In addition, the measured temperatures are shown to be in fairly good agreement with the calculated one using the value of α_h = 150 W/m^{2}K.

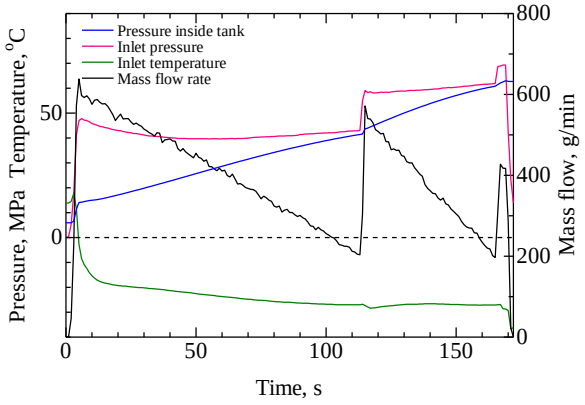

Fig. 6(a) Input data in filling test

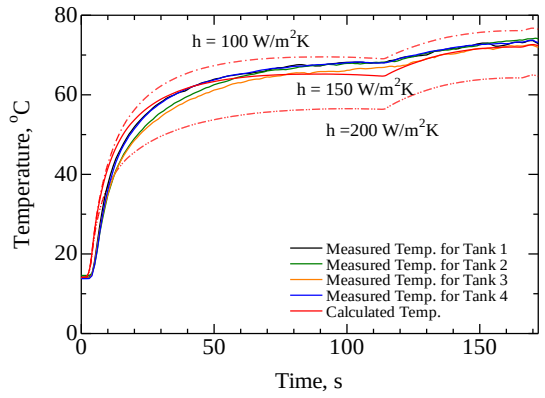

Fig. 6(b) Comparison between measured and estimated temperatures up to 70 MPa for type IV with 31 L (Run #3)

The same tanks as the Run #3 are used to carry out the fill test of Run #4 listed in Table 1. Figure 7(a) shows a measured inlet precooled temperature ranging from mainly about - 20 to - 30 °C and measured pressure in the 31 L test tanks during filling to 70 MPa at a constant flow rate through a compressor, and also Fig. 7(b) shows measured temperatures for the four identical tanks and calculated results using different heat transfer coefficients of α_h = 25 to 50 W/m^{2}K. As it takes 793 s for the tanks to be filled, we make the values of α_h much smaller than that for filling time of 172 s. Figure 7(b) shows that the good agreement between the measured and estimated temperatures except for the time beyond 600 s and that the difference in the temperatures among four tanks becomes negligibly smaller than that for the case of fast filling, since the difference in the mass flow rate for very slow filling time of 793 s might be negligibly small.

Figure 8(a) shows a measured inlet precooled temperature ranging from about - 20 to - 30 °C, a change

in mass flow rate and the measured pressure in 40 L test tank during filling to 70 MPa using three hydrogen banks, and also Fig. 8(b) shows measured temperatures and calculated results using a heat transfer coefficient of α_h = 200 W/m^{2}K. It is apparent from Fig. 8(b) that the calculated temperature agrees well with the measured temperature until 120 s, but after 120 s, the estimated temperature becomes consistently higher than the measured temperature. This reason may come mainly from the ignorance of heat loss through the metals at both ends of the tank and from adopting a smaller heat transfer coefficient in spite of an increase in mass flow rate by switching the banks. But, the temperature difference between the measured and estimated temperatures is only about 5 K at the end of the filling time, which may be allowed within a tolerance band. Figure 8(c) shows the temperature change in the liner and CFRP with time. It may be noticed from Fig. 8(c) that the temperature does not penetrate into the end of the CFRP surface and most of heat from hydrogen is stored as internal energy within the liner. In addition, for a fast fill shorter than 3 min, the environmental condition has no effect on the hydrogen temperature, because the temperature change does not reach the end of the wall as shown in Fig. 8(c). It should be noticed that a position at which 1 % of the temperature change on the surface occurs, is given by $\delta = 3.64\sqrt{at}$ [m], and for example δ = 39.7 mm for CFRP with a = 0.66 x 10^{-6} m^2/s at 180 s.

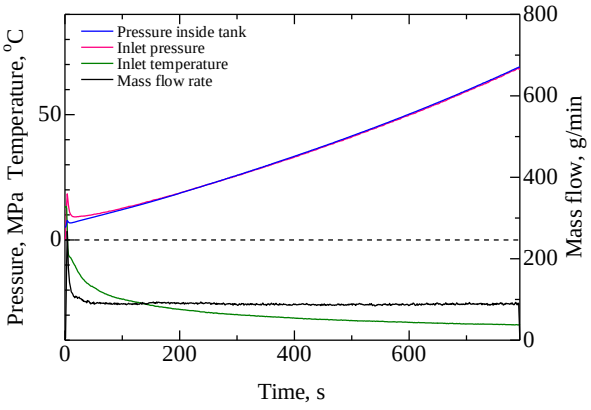

Fig. 7(a) Input data in filling test

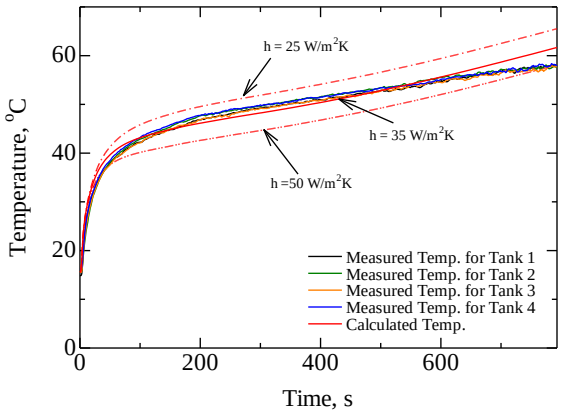

Fig. 7(b) Comparison between measured and estimated temperatures up to 70 MPa for type IV with 31 L (Run #4)

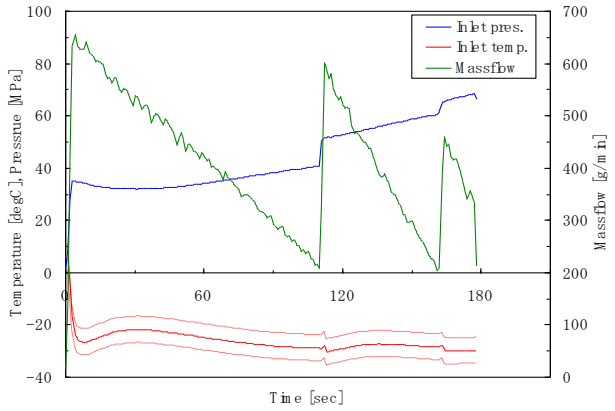

Fig. 8(a) Input data in filling test

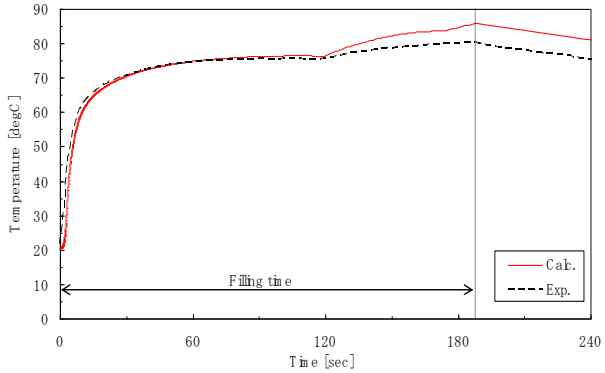

Fig. 8(b) Comparison between measured and estimated temperatures up to 70 MPa for type IV with 40 L (Run #5)

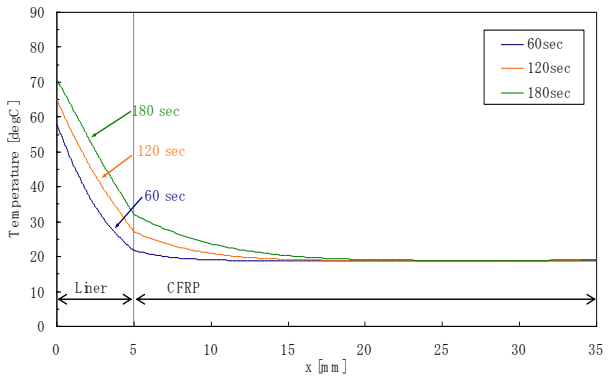

Fig. 8(c) Temperature change in the liner and CFRP with time

Figure 9(a) shows a measured inlet precooled temperature ranging from about - 20 to - 30 °C, a change in mass flow rate and measured pressure in a 39 L test tank during filling to 70 MPa using three hydrogen banks, and also Fig. 9(b) shows measured temperatures and calculated results using different heat transfer coefficients of α_h = 150 W/m^{2}K. It is revealed from Fig. 9(b) that the estimated temperature agrees well with the measured temperature over the filling time, while the estimated temperature has a slightly different trend from the measured temperature. This reason may come mainly from the adoption of a slightly smaller heat transfer coefficient and also adopting a constant heat transfer coefficient in spite of an increase in mass flow rate by switching the banks. But, the temperature difference

between the measured and estimated temperatures is only about 5 K at the end of filling time, which may be allowed within the tolerance bound of 5 K. Figure 9(c) shows the temperature change in the liner and CFRP with time during the filling process. Figure 9(c) shows that the temperature rise for Run #6, penetrates deeper into the CFRP than that for Run #5 at the same time due to the higher thermal diffusivity. If the liner has larger thermal conductivity like aluminum, the temperature change penetrates deeper into the CFRP, resulting in a lower hydrogen temperature in the tank.

Figure 9(d) shows the amount of supplied enthalpy, of stored internal energy in the tank and the heat loss calculated from Eq.(1) during filling process and also the calculated heat loss from Eq.(6). On comparison of the heat losses from Eqs. (1) and (6), it is found that both the heat losses are totally overlapped over the fill time. This fact means that the stored process of hydrogen can be correctly made from thermal energy point of view, although the trend in their temperature changes is slightly different. In addition, it is found from Fig. 9(d) that the stored energy as internal energy in the tank is estimated to be about 90 % of the supplied enthalpy, and then the value of supplied energy minus stored energy in the tank, namely, $\Delta H(t) - \Delta U(t)$ is totally overlapped on the heat loss to the wall calculated from Eq.(6). It should be noted that about 10 % of the supplied energy is transferred in the wall.

Finally, it may be worth mentioning that Japan Automobile Research Institute (JARI) [16] analyzed their data of measured temperatures using the same software and reported that the predicted values are in good agreement with the measured one. In addition, the measured temperature at the gas-inlet given by the red line may correspond to the supplied gas temperature immediately after the gas is released into the tank and that the temperature at the end of filling time quickly merged into other measured temperatures at the other locations in the tank.

3.2 Validation of well stirred condition assumption

Dicken and Meridas [5] experiment shows that the measured temperatures at 63 different locations in the tank seem to be almost uniform except for the inlet zone which is influenced by the supplied hydrogen and the zone near the surface, where heat transfer takes place between surface and hydrogen. On the other hand, Woodfield et al. [13] measured the average heat transfer coefficient during filling into a small tank and discharging gas from the tank. They [13] mentioned that during filling hydrogen, the heat transfer coefficients vary from 100 to around 450 W/m^{2}K depending on filling mass flow rate from 0.1 to 0.6 g/s, and then their values are strongly influenced by the locations and is increased as the location becomes farther from the inlet. On the other hand, when the hydrogen is discharged, the heat transfer coefficients are almost independent of the location and its values continuously decrease from 200 to around 50 W/m^{2}K as the mass flow rate decreases from 0.6 to 0.1 g/s. Although the mass flow rate is almost identical between filling and discharging, the heat transfer coefficients behave with very different trends.

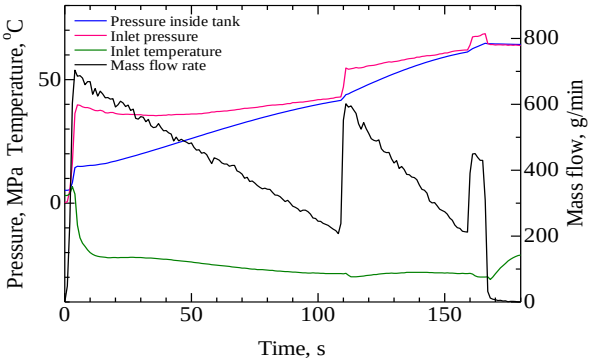

Fig. 9(a) Input data in filling test

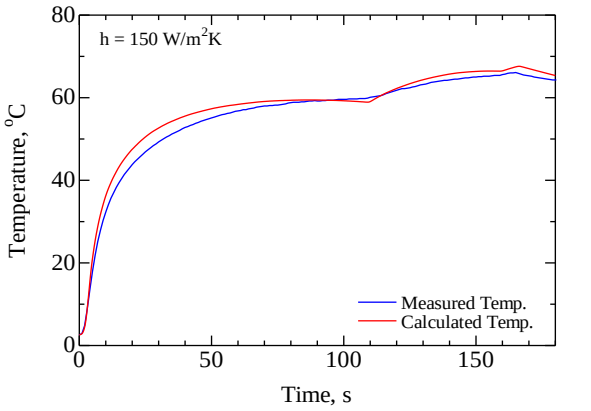

Fig. 9(b) Comparison between measured and estimated temperatures up to 70 MPa for type IV with 39 L (Run #6)

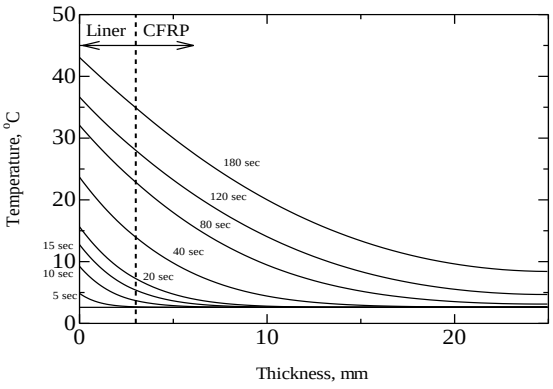

Fig. 9(c) Temperature change in the liner and CFRP with time

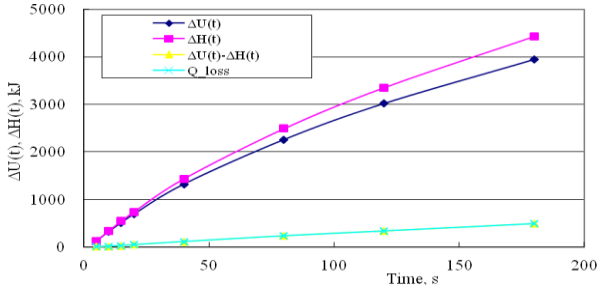

Fig. 9(d) Temperature change in the liner and CFRP with time

This different behavior is due to different flow situations.

It is found from Figs. 4 to 9 that all the measured temperatures obtained in the filling tests of #1 to #6 can be well predicted by employing the value of α_h smaller than α_h = 200 W/m^{2}K as an average one, although the heat transfer coefficient chaotically changes with time and also position. In addition, it may be worth noticing that the value of α_h = 150 or 200 W/m^{2}K is employed for the mass flow rates from 3 to 10 g/s, which are much smaller than that recommended for 0.1 to 0.6 g/s by Woodfield et al. [13]. This fact may support the assumption that the temperature in the tank is well stirred for the case in the present study and is uniformly distributed as a special average for any particular value of time.

4. APPLICATION OF MODEL PREDICTION TO FILLING PROCEDURE

The hydrogen temperature during the filling process depends on the five other parameters as given by Eq.(12), mentioned before. Setting T_f = 85°C, for example to keep the upper-limit due to the safety requirement, one can obtain in place of Eq. (12):

$$f_1(p_o, T_o, p_f, T_f = 85, t, T_{in}) = 0 \tag{13}$$

In other words, in the case of a fixed final temperature such as T_f = 85 °C, any one from five parameters during the filling process can be determined using other four independent parameters. Therefore, a required parameter such as the filling time or the temperature of the filling gas in Eq.(13) can be explicitly expressed using other independent parameters, that is:

$$t = g_1(p_o, T_o, p_f, T_{in}) \tag{14-a}$$

$$T_{in} = g_2(p_o, T_o, p_f, t) \tag{14-b}$$

The functional forms for Eq. (14) are rather difficult to derive analytically because the energy equation for the gas in the vessel and governing equation for heat conduction through the wall of the vessel are coupled and then relations between them become non-linear. Therefore, for a given composite vessel, for which all concerned values such as volume, surface area and thermal properties are known, we first calculate the values of filling time t and temperature T_{in} for an initial condition (p_o and T_o) by applying numerical computing code based on the Woodfield et al. model [4]. We repeat this calculation for the range of the initial conditions as given in Table 1, and specific tanks given in Table 2, and then obtain each combination of filling time t and temperature T_{in} for the corresponding initial condition. We apply a regression method to the calculated data set of p_o, T_o, p_f, t and T_{in} values given by Eq. (13), resulting in an explicit functional form given by Eq. (14).

It is worth mentioning that from an engineering point of view the approximate equations shown in Eq. (14) are of importance to quickly determine the filling time against the initial condition and the temperature T_{in}, which is already set at a hydrogen station. In order to design precooling equipment, we need the precooling value for T_{in} for the required filling time and the initial condition.

Recently, Monde et al. [18] derived concrete forms for Eq.(14) based on calculated results for a wide range of initial conditions, which may meet actual operating conditions of FCV as follows:

$$t = \left(\sum_{i=0}^{3} \sum_{j=0}^{1} \sum_{k=0}^{1} \sum_{l=0}^{2} C_{i,j,k,l} \left(\frac{T_o}{T_n} \right)^i \left(\frac{P_o}{P_f} \right)^j P_f{}^k \left(\frac{T_{in}}{T_n} \right)^l \right)^2 \tag{15-a}$$

$$\frac{T_{in}}{T_n} = \sum_{i=0}^{2} \sum_{j=0}^{2} \sum_{k=0}^{2} C_{i,j,k} \left(\frac{T_o}{T_n} \right)^i \left(\frac{P_o}{P_f} \right)^j t^{\frac{k}{2}} + \frac{1}{P_f} \sum_{l=0}^{2} \sum_{m=0}^{2} C_{l,m} \left(\frac{T_o}{T_n} \right)^l t^{\frac{m}{2}} \tag{15-b}$$

The order of polynomial terms is determined to meet an effect of each independent parameter on the required parameter. Monde et al. [18] reported that Eq.(15-a) can predict the simulated time at about 2500 points selected from the actual expected range of (p_o, T_o, p_f, T_{in}) combination within an accuracy of smaller than 5 % relative deviation, which may be allowable for filling a hydrogen tank, and predict the simulated temperature, T_{in} at 3000 points for a type III vessel and 2160 points for a type IV vessel selected from the actual expected range of (p_o, T_o, p_f, t) with a standard deviation of 1.5 K.

5. CONCLUSIONS

Available test data obtained in the filling tests are analyzed by the developed software based on the Monde et al. model [3, 4]. The parameters concerned with filling process are clearly mentioned to be six in which four independent parameters under the condition of T_f = 85 ℃ can determine other required value, such as the filling time or precooled temperature. The temperature rise during filling process is well predicted and is in good agreement with the estimated temperature. The developed software is available to simulate the temperature rise at any given combination from which Eq.(15) can be derived for any specific tank. Explicit expressions such as Eq. (15) will be needed to construct hydrogen stations and to practically operate the filling process.

Nomenclature

a – thermal diffusivity of solid
A – inside surface area of tank
Bi– Biot number (= $h\delta/\lambda$)
c – specific heat for solid
c_p – constant pressure specific heat for gas
h – specific enthalpy
ΔH –Increase in total enthalpy of supplied hydrogen
l – total thickness of wall
m– mass flow rate into tank
p – gas pressure
Q – heat loss into wall
t – time
T_g – gas temperature
T – temperature
ΔU –Increase in total internal energy of hydrogen

u – specific internal energy

V – tank volume

Greek

α – convection heat transfer coefficient

δ – thickness of material

λ – thermal conductivity

Π – dimensionless parameter

ρ - density

Subscript

e – outer surface of tank

f – final condition

g – gas

h – inner surface of tank

in – property or quality at inlet

n – reference

o – initial condition

s – solid

w – wall at inner surface

ACKNOWLEDGMENTS

Authors would like to express their appreciation to New Energy and Industrial Technology Development Organization (NEDO) for financial support to this research and also to the Japan Automotive Research Institute (JARI) and some companies concerned for the disclosure of their data.

References

[1] Iida K., Trends in hydrogen and fuel cell efforts by the Japanese government, FY 2010 JHFC International Seminar, (2011. 28 - March. 1) at Tokyo International Forum.

[2] Okazaki K., JHFC Phase 2 Summary (FY2006-2010), FY 2010 JHFC International Seminar, (2011. Feb. 28 - March. 1) at Tokyo International Forum.

[3] Monde M., Mitsutake Y., Woodfield P. L., Maruyama S., Characteristics of Heat Transfer and Temperature Rise of Hydrogen during Rapid Hydrogen Filling at High Pressure, *Heat Transfer – Asian Research*, Vol. 36 (2007) pp. 13-27.

[4] Woodfield P. L., Monde M., Takano T., Heat transfer characteristics for practical hydrogen pressure vessels being filled at high pressure, J. of Thermal Science and Technology, 3(2) (2008), pp.241-53.

[5] Dicken C. J.B., Merida W., Measured effects of filling time and initial mass on the temperature distribution within a hydrogen cylinder during refueling, J. of Power Sources, 165 (2007), pp.324-336.

[6] Dicken C. J. B, Merida W., Modeling the transient temperature distribution within a hydrogen cylinder during refueling, J. of Numerical Heat Transfer Part A 53 (2008), pp.1-24.

[7] Liu Y., et al., Experimental studies on temperature rise within a hydrogen cylinder during refueling, International Journal of Hydrogen Energy, 35 (2010), 2627-2632.

[8] Heitsch M., Baraldi D., Moretto P., Numerical investigations on the fast filling of hydrogen tanks, International Journal of Hydrogen Energy, 36 (2011), pp.2606-2612.

[9] Zhao L., et al., Numerical simulation of temperature rise within hydrogen vehicle cylinder during refueling, International Journal of Hydrogen Energy, 35 (2010), 8092-8100.

[10] Yang J. C., A thermodynamic analysis of refueling of a hydrogen tank. International Journal of Hydrogen Energy, 34 (2009), 6712-6721.

[11] Maus S., et al., Filling procedure for vehicles with compressed hydrogen tanks, International Journal of Hydrogen Energy, 33 (2008), pp.4612-4621.

[12] Zheng, J., et al., An optimized control method for a high utilization ratio and fast filling speed in hydrogen refueling stations, International Journal of Hydrogen Energy, 35 (2010), 3011-3017.

[13] Woodfield P. L., Monde M., Mitsutake Y., Measurement of average heat transfer coefficients in high-pressure vessel during charging with hydrogen, nitrogen or argon gas, *J. of Thermal Science and Engineering*, Vol.2, No.2, (2007), pp.180-190.

[14] Lee, B. I. and Kesler, M. B., A generalized thermodynamic correlation based on three-parameter corresponding states, *AIChE Journal* 21 (1975) 510-527.

[15] Perry, R. H., Green, D. W., and Maloney, J. O., *Perry's Chemical Engineers' Handbook, 7th Edition*, McGraw-Hill, USA, pp. 2-224 – 2-245, 1997.

[16] Private communication on temperature change with time during filling hydrogen with JARI, (2008).

[17] Ranong, C., Maus, S., Hapke, J. , Fieg, G. and Wenger, D., Approach for the determination of heat transfer coefficients for filling processes of pressure vessels with compressed gaseous media, Heat Transfer Engineering, 32 (2), (2011), pp.127-132.

[18] Monde, M., Tanaka, S. and Takano, T., Prediction of filling time and temperature of precooled hydrogen during filling of hydrogen into a high-pressure tank, Proc. of SAE 2010-32-0127, Small Engine Technology Conf., Linz, Austria, (Sept. 28-30, 2010).